



## Bismuth-induced phase control of GaAs nanowires grown by molecular beam epitaxy

Zhenyu Lu, Zhi Zhang, Pingping Chen, Suixing Shi, Luchi Yao, Chen Zhou, Xiaohao Zhou, Jin Zou, and Wei Lu

Citation: [Applied Physics Letters](#) **105**, 162102 (2014); doi: 10.1063/1.4898702

View online: <http://dx.doi.org/10.1063/1.4898702>

View Table of Contents: <http://scitation.aip.org/content/aip/journal/apl/105/16?ver=pdfcov>

Published by the [AIP Publishing](#)

---

### Articles you may be interested in

[Vapor liquid solid-hydride vapor phase epitaxy \(VLS-HVPE\) growth of ultra-long defect-free GaAs nanowires: Ab initio simulations supporting center nucleation](#)

*J. Chem. Phys.* **140**, 194706 (2014); 10.1063/1.4874875

[Quality of epitaxial InAs nanowires controlled by catalyst size in molecular beam epitaxy](#)

*Appl. Phys. Lett.* **103**, 073109 (2013); 10.1063/1.4818682

[Ferromagnetic \(Ga,Mn\)As nanowires grown by Mn-assisted molecular beam epitaxy](#)

*J. Appl. Phys.* **113**, 144303 (2013); 10.1063/1.4799624

[Facet structure of GaAs nanowires grown by molecular beam epitaxy](#)

*Appl. Phys. Lett.* **91**, 083106 (2007); 10.1063/1.2769401

[Anisotropy of selective epitaxy in nanoscale-patterned growth: GaAs nanowires selectively grown on a Si O<sub>2</sub>-patterned \(001\) substrate by molecular-beam epitaxy](#)

*J. Appl. Phys.* **98**, 114312 (2005); 10.1063/1.2132093

---

**Pure Metals • Ceramics**  
**Alloys • Polymers**  
in dozens of forms

**Goodfellow**

Small quantities *fast* • Expert technical assistance • 5% discount on online orders



## Bismuth-induced phase control of GaAs nanowires grown by molecular beam epitaxy

Zhenyu Lu,<sup>1</sup> Zhi Zhang,<sup>2</sup> Pingping Chen,<sup>1,a)</sup> Suixing Shi,<sup>1</sup> Luchi Yao,<sup>1</sup> Chen Zhou,<sup>2</sup> Xiaohao Zhou,<sup>1</sup> Jin Zou,<sup>2,3</sup> and Wei Lu<sup>1,a)</sup>

<sup>1</sup>National Laboratory for Infrared Physics, Shanghai Institute of Technical Physics, Chinese Academy of Sciences, 500 Yu-Tian Road, Shanghai 200083, China

<sup>2</sup>Materials Engineering, The University of Queensland, St. Lucia, Brisbane, Queensland 4072, Australia

<sup>3</sup>Center for Microscopy and Microanalysis, The University of Queensland, Brisbane, Australia

(Received 25 July 2014; accepted 8 October 2014; published online 20 October 2014)

In this work, the crystal structure of GaAs nanowires grown by molecular beam epitaxy has been tailored only by bismuth without changing the growth temperature and V/III flux ratio. The introduction of bismuth can lead to the formation of zinc-blende GaAs nanowires, while the removal of bismuth changes the structure into a 4H polytypism before it turns back to the wurtzite phase eventually. The theoretical calculation shows that it is the steadiest for bismuth to adsorb on the GaAs(111)<sub>B</sub> surface compared to the liquid gold catalyst surface and the interface between the gold catalyst droplet and the nanowire, and these adsorbed bismuth could decrease the diffusion length of adsorbed Ga and hence the supersaturation of Ga in the gold catalyst droplet. © 2014 AIP Publishing LLC. [<http://dx.doi.org/10.1063/1.4898702>]

III-V semiconductor nanowires have attracted great interests for more than a decade due to their potential applications in electronics,<sup>1</sup> photonics,<sup>2</sup> and sensors.<sup>3</sup> Many of these applications are based on a low defect density and a high crystal quality of nanowires, because the crystallographic properties have a significant effect on the carrier lifetime,<sup>4</sup> the electrical energy band,<sup>5</sup> and the transport properties.<sup>6</sup> Therefore, a precise control of nanowire structures is required before their applications come true. During the past decade, many methodologies have been proposed to tailor the crystal structure grown by the vapor-liquid-solid (VLS) mechanism. Joyce<sup>7</sup> proposed different combinations of the growth temperature and V/III flux ratio to tune the phase perfection, while the phase transition between wurtzite (WZ) and zinc blende (ZB) structures has been controlled only by changing the V/III flux ratio<sup>8</sup> or only by varying the growth temperature.<sup>9</sup> Alternative approach is by such additive atoms as antimony<sup>10</sup> or zinc<sup>11,12</sup> to tune the phase structure of GaAs or InP nanowires.

It is now well accepted that there are at least three parameters that influence the polytypism in particle-assisted III-V nanowire growth: supersaturation, interface energies, and the contact angle.<sup>13</sup> For example, realizing single-phase growth often needs high supersaturation conditions for pure WZ structure, or low supersaturation for pure ZB structure.<sup>13</sup> Moreover, the large contact angle and the lower surface energy of the catalyst particle will favor the formation of ZB crystal phase.<sup>14</sup> The growth temperature and V/III flux ratio usually affect the crystal structure of nanowires by changing supersaturation.<sup>9</sup> Besides the growth temperature and V/III flux ratio, the introduction of additive atoms is also able to control the crystal structure of nanowires via adjusting the above mentioned three parameters. Algra *et al.* demonstrated that they can control the crystal structure of InP nanowires by impurity dopants and ascribed it to the modulation of

interface energies.<sup>12</sup> Meanwhile, the ZB phase of GaAsSb nanowires was found to be favorably formed after the introduction of Sb, which can be explained by the changing of supersaturation very well.<sup>10</sup> Nonetheless, controlling crystal phase in III-V nanowires using the additive atom still remains challenging and requires further investigations to understand the fundamental growth mechanism.

In this study, we have grown GaAs nanowires by molecular beam epitaxy (MBE), in which the crystal structure is tailored by alternatively adding or removing bismuth. By the qualitative analysis, we attribute the phase transition to the bismuth which decreases the supersaturation in the alloy droplet by impeding the diffusion of adsorbed Ga on the substrate to the growth front.

GaAs nanowires were grown in the bismuth ambient via the VLS growth approach on GaAs(111)<sub>B</sub> substrates in a Riber 32 MBE system with the As<sub>4</sub> source. The growth temperature was 420 °C and the As<sub>4</sub>/Ga beam equivalent pressure (BEP) ratio was set at 23, with the Ga BEP of  $2.0 \times 10^{-7}$  Torr and the As<sub>4</sub> BEP of  $4.6 \times 10^{-6}$  Torr. These growth conditions were set to grow pure WZ structured GaAs nanowires<sup>15,16</sup> when no bismuth exists in the ambient. The bismuth BEP was maintained at  $2.0 \times 10^{-7}$  Torr. After 50-min growth, the bismuth shutter was closed and the growth of GaAs nanowires continued for another 10 min without bismuth in the ambient. Morphological characterization of GaAs nanowires was carried out in a JEOL 7800F scanning electron microscopy (SEM) operating at 10 kV, and their crystallographic structure was analyzed in detail by a Philips Tecnai F20 and a FEI Tecnai F30 transmission electron microscopy (TEM) operating at 200 kV and 300 kV, respectively. The Tecnai F20 TEM is equipped with an X-ray energy dispersive spectroscopy (EDS) for the compositional analysis. The nanowires for TEM characterization were ultra-sonicated off from the substrates in ethanol and then dispersed onto holey carbon films supported by Cu mesh grids.

<sup>a)</sup>Electronic addresses: ppchen@mail.sitp.ac.cn and luwei@mail.sitp.ac.cn

Figure 1(a) is a SEM image of a typical GaAs nanowire, showing its tapered morphology. Figure 1(b) is a TEM image of the tip section of a nanowire, and Figs. 1(c) and 1(d) are high-resolution TEM images taken from different sections of the nanowire shown in Fig. 1(b). Figures 1(c) and 1(d) depict the phase information of the top part grown without bismuth (defined as GaAs-II) and the phase information of the bottom part grown with bismuth in the ambient (defined as GaAs-I), respectively. As can be seen from the selected area electron diffraction [SAED, insets in Figs. 1(c) and 1(d)], the GaAs-I is of ZB structure [shown in Fig. 1(d)], which was obtained only by adding bismuth atoms without changing any other conditions. In contrast, the GaAs-II shows an impure 4H polytypism followed by the WZ structure [shown in Fig. 1(c)]. These two findings indicate that the introduction of bismuth can control the crystal structure of GaAs nanowires: the presence of bismuth favors the formation of ZB structure, while the removal of bismuth changes the ZB structure to a 4H polytypism and finally back to the WZ structure.

In order to further investigate the effect of bismuth on the control of crystal structure of GaAs nanowires, we have grown the GaAs nanowires with five GaAs-I inserts with following features in the inserts. Each GaAs-I insert was grown for 1 min, and from the bottom to the top of nanowire, the bismuth BEP for each insert increased gradually from  $7.5 \times 10^{-8}$  Torr to  $4.8 \times 10^{-7}$  Torr, as shown in Fig. 2(a). After each insert, the GaAs-II section was grown for 9 min with the bismuth source switched off. Throughout the growth, the growth temperature and the As/Ga BEP ratio were kept at  $420^\circ\text{C}$  and approximately 20, respectively.

Since all GaAs-I inserts were grown in a single nanowire, we can explore the mechanism of crystal-structure transformation induced by bismuth, excluding the effect of other growth parameters, such as growth temperature and V/III flux ratio, on the crystal structure. Since the third insert

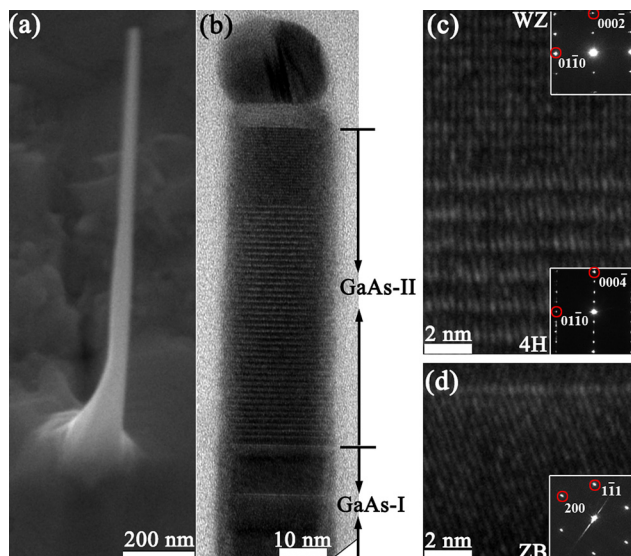


FIG. 1. (a) The  $30^\circ$ -tilted SEM image of a typical GaAs nanowire grown in the bismuth ambient. (b) The TEM image near the tip section of the GaAs nanowire, including the GaAs-I and the GaAs-II. (c) The 4H polytypism followed by the WZ structure in GaAs-II and (d) the ZB structure of GaAs-I, in which the insets of SAED patterns verify the corresponding crystal structure. The two circles in the bottom inset of (c) show the (0110) and (0004) diffraction points for a 4H polytype phase.

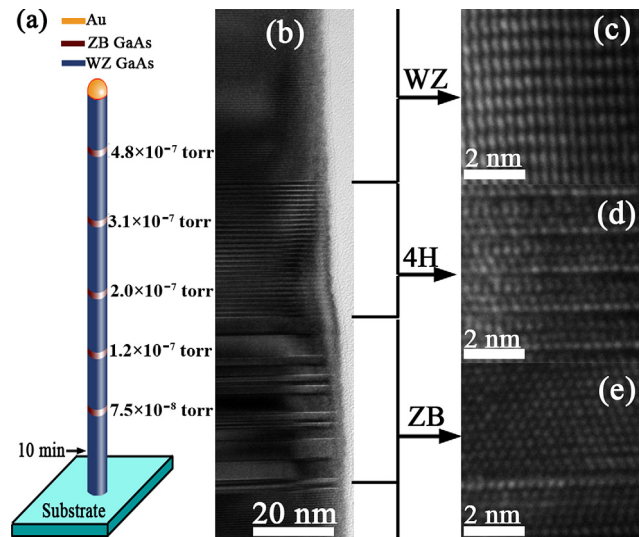


FIG. 2. (a) The scheme of GaAs nanowire with five GaAs-I inserts to depict the growth process. (b) The TEM image showing the structural transition from WZ to ZB and back to WZ. The 4H segment follows the ZB segment. (c)–(e) correspond to the high-resolution TEM images of the WZ segment, the 4H polytype section and the ZB GaAs-I insert in the GaAs nanowire, respectively.

from the top was grown with the bismuth BEP of  $2.0 \times 10^{-7}$  Torr (identical to the previous case), we first focus on this GaAs-I insert to see whether the transition of crystal structure has been repeated. Figures 2(b)–2(d) show the detailed TEM investigations. As expected, before the bismuth was introduced to the growth ambient, GaAs nanowires present a pure WZ structure. Once introducing bismuth, the transition from the pure WZ structure to the twinned ZB structure (GaAs-I) happens abruptly [as shown in Figs. 2(b) and 2(e)]. The close of bismuth source causes the expected formation of GaAs-II, which is a 4H polytypism followed by the WZ structure [refer to Figs. 2(c) and 2(d)]. The similar phase transition has been also reported by Dheeraj *et al.*<sup>10</sup> Their transition was caused by the introduction of antimony and the ZB segment was a ZB structured GaAsSb insert. However, the EDS result of our GaAs-I shown in Fig. 3(a)

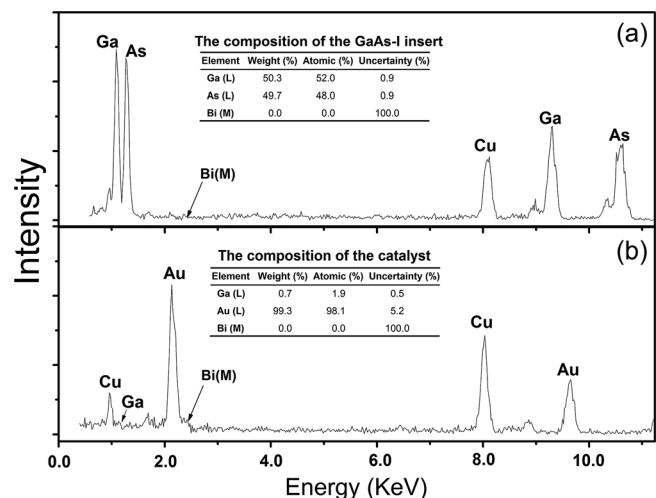


FIG. 3. The EDS results showing the composition of (a) the GaAs-I insert and (b) the catalyst in the nanowire. Both spectra indicate no distinct existence of bismuth.



reveals no existence of the bismuth in GaAs nanowires. A further EDS measurements were both performed in the gold catalyst [as shown in Fig. 3(b)] and in the neck section formed during the cooling down, and again no bismuth was detected. Therefore, it is suggested that, in our case, the bismuth does not participate in the formation of nanowires like antimony.

Figures 4(a)–4(e) show the structural characteristics of the five GaAs-I inserts (between the two lines) taken from a typical nanowire. Under the bismuth BEP conditions of  $7.5 \times 10^{-8}$  Torr and  $1.2 \times 10^{-7}$  Torr, both GaAs-I inserts do not present a ZB phase. In these cases, only stacking faults are formed in the WZ structure, as shown in Figs. 4(a) and 4(b). However, when bismuth BEP is increased to the amount comparable with gallium [Fig. 4(c)], the expected ZB structured GaAs-I is obtained with some twins. With further increasing bismuth, the transition from WZ to ZB happens, as shown in Figs. 4(d) and 4(e). The pure ZB insert is

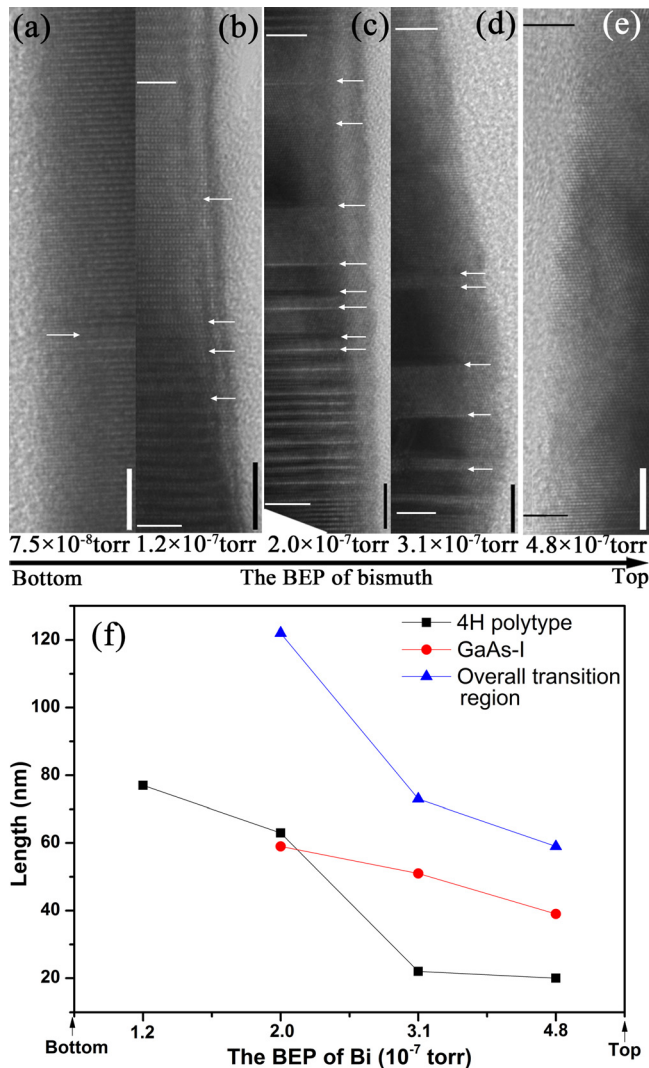


FIG. 4. The structure variation of the transition region with the BEP of bismuth. (a)–(e) correspond to the TEM images of the GaAs-I inserts (between the two lines) in the five transition regions from the bottom to the top in one single nanowire. The arrows in (a) and (b) mark the positions of stacking faults and those in (c) and (d) the position of the twinned ZB. The BEPs of bismuth for each transition region are listed below, respectively. The scale bar is 5 nm. (f) Length variation of the 4H polytype section, the GaAs-I insert, and the whole transition region with the content of bismuth.

obtained finally under the bismuth BEP condition of  $4.8 \times 10^{-7}$  Torr. According to these experimental results, it can be noted that the increase of bismuth BEP can reduce the density of twin defects in the GaAs-I inserts. Above the GaAs-I, the 4H polytype phase forms due to the close of bismuth, except the case where the amount of bismuth is smallest [refer to Fig. 4(a)]. Figure 4(f) depicts the length variation of the transition region, including the 4H polytype section and the GaAs-I insert, with the amount of bismuth. From the bottom to the top, the length of the 4H polytype section decreases with increasing bismuth. The same trend holds for the ZB GaAs-I insert and hence for the overall length of the 4H polytype section and the ZB GaAs-I insert.

In order to clarify the reason for the phase transformation caused by bismuth, two issues need to be addressed. The first issue is that why we cannot detect Bi in the nanowire and catalyst. The second issue is that why the introduction of Bi could tailor the structure of nanowire. To address the first issue, we noted that in the two dimensional growth, bismuth has a strong tendency to surface segregation, so that it is difficult for bismuth to be incorporated into the surface to form GaAsBi film under conventional GaAs film growth conditions.<sup>17,18</sup> In our case, we cannot find any bismuth on the post-grown GaAs substrates by EDS investigation. Further theoretical calculations by the first principle show that the energies of adsorption of bismuth on the GaAs(111)<sub>B</sub> surface, on the liquid gold catalyst surface, and at the interface between the gold catalyst droplet and the nanowire are 4.11 eV, 3.13 eV, and 2.49 eV, respectively. The energy of adsorption  $E_{ad}$  is defined as<sup>19</sup>

$$E_{ad} = \frac{E_{bf} + \sum_{i=1}^n E_i - E_{af}}{n}, \quad (1)$$

where  $E_{af}$  represents the total energy of the system after atoms are adsorbed,  $E_{bf}$  is the total energy of the system without adsorbed atoms,  $E_i$  is the energy of an isolated atom, and  $n$  is the total number of adsorbed atoms. According to Eq. (1), positive  $E_{ad}$  means that the adsorption is an exothermic process, and the larger the  $E_{ad}$  of atoms on a specific surface, the more steadily they stay there. Therefore, the above calculated energies of adsorption reveal that bismuth atoms prefer to stay on the surface of GaAs(111)<sub>B</sub> substrate, while it is difficult for them to reach the interface between the gold catalyst droplet and the nanowire to participate in the nucleation there. In this regard, bismuth cannot be detected in the ZB GaAs-I inserts as well as in the gold catalysts.

Then, how does the bismuth tailor the crystal structure of nanowires? It has been reported that the additive zinc can lower the liquid-solid step energy for ZB structure,<sup>12</sup> while the additive antimony will increase the equilibrium concentration of Ga in the Au-Ga alloy droplet.<sup>20,21</sup> However, as is mentioned above, bismuth preferentially adsorbs on the substrate surface, and no bismuth is detected in the Au-Ga alloy droplet. These two facts suggest that bismuth should not be possible to get into the Au-Ga alloy droplet to lower the liquid-solid step energy (like zinc), or to increase the equilibrium concentration of Ga in the droplet (like antimony). To understand the role of bismuth, we note that when growing

GaAsBi film by MBE, bismuth is easy to become a “bonding anti-surfactant,”<sup>22,23</sup> which occupies the substitutional surface sites and reduces the surface diffusion length of adatoms on the substrate surface. Considering that, in our case, bismuth prefers to stay on the surface of GaAs(111)<sub>B</sub> substrate, the bismuth might also act as the “bonding anti-surfactant,” and in turn decreases the diffusion length of Ga atoms. Generally, the majority of Ga atoms that migrate to the gold catalyst come from the diffusion of Ga atoms on the substrate in the MBE system. Since the diffusion length of Ga atoms decreases, the number of Ga atoms that diffuse from the substrate to the gold catalyst droplet declines and accordingly the supersaturation of Ga decreases. After the bismuth source is closed, bismuth atoms are desorbed gradually from the substrate and the diffusion length of Ga increases again. This makes the supersaturation increase gradually. It is well accepted that the supersaturation for the formation of WZ nanowires has to be high enough while the supersaturation for ZB nanowires needs to be low enough, and the median supersaturation between the former two gives the possibility of forming the 4H polytypism.<sup>24</sup> Therefore, the introduction of bismuth causes the formation of ZB GaAs-I inserts, while the crystal structure changes to the 4H polytypism and eventually back to ZB phase after the removal of bismuth.

With increasing bismuth, more “bonding anti-surfactants” form on the substrate, causing a strong suppression of Ga diffusion on the substrate, and in turn less concentration of Ga in the alloy droplet. As a result, the increase of bismuth partial pressure lowers the growth rate of nanowires, and accordingly the length of ZB GaAs-I inserts decreases with increasing bismuth. Similarly, since more bismuth causes less concentration of Ga in the gold catalyst, the supersaturation decreases more greatly and hence the crystal structure of ZB GaAs-I inserts becomes purer with increasing bismuth partial pressure.

In conclusion, we have achieved to tailor the crystal structure of GaAs nanowires between ZB and WZ phases by adding or removing the bismuth. However, bismuth does not participate in the formation of nanowires. We have found that the ZB GaAs-I insert forms with the bismuth in the ambient, while removing the bismuth changes the crystal structure to the 4H polytypism and finally back to the WZ structure. The theoretical calculation reveals that bismuth prefers to stay on the GaAs(111)<sub>B</sub> surface for its largest adsorption energy, comparing to the other locations such as the gold catalyst surface and the interface between the gold catalyst and the nanowire. These adsorbed bismuth could decrease the diffusion length of adsorbed Ga and hence the supersaturation of Ga in the gold catalyst droplet, resulting in the transition from the WZ structure to the ZB structure.

This project was supported by the National Basic Research Program of China (Grant No. 2011CB925604), the National Science Foundation of China (Grant Nos. 61376015, 91321311, 11334008, and 91121009), Shanghai Science and Technology Foundation (Grant Nos. 13JC1405901 and 13ZR1446200), and Australian Research Council. Australian Microscopy & Microanalysis Research Facility is gratefully acknowledged for providing microscopy facilities for this study.

- <sup>1</sup>C. Thelander, P. Agarwal, S. Brongersma, J. Eymery, L. F. Feiner, A. Forchel, M. Scheffler, W. Riess, B. J. Ohlsson, U. Gosele, and L. Samuelson, *Mater. Today* **9**, 28 (2006).
- <sup>2</sup>F. Qian, Y. Li, S. Gradecak, D. L. Wang, C. J. Barrelet, and C. M. Lieber, *Nano Lett.* **4**, 1975 (2004).
- <sup>3</sup>P. Offermans, M. Crego-Calama, and S. H. Brongersma, *Nano Lett.* **10**, 2412 (2010).
- <sup>4</sup>P. Parkinson, H. J. Joyce, Q. Gao, H. H. Tan, X. Zhang, J. Zou, C. Jagadish, L. M. Herz, and M. B. Johnson, *Nano Lett.* **9**, 3349 (2009).
- <sup>5</sup>P. Kusch, S. Breuer, M. Ramsteiner, L. Geelhaar, H. Riechert, and S. Reich, *Phys. Rev. B* **86**, 075317 (2012).
- <sup>6</sup>S. A. Dayeh, *Semicond. Sci. Technol.* **25**, 024004 (2010).
- <sup>7</sup>H. J. Joyce, Ph.D. thesis, The Australian National University, Canberra, 2009.
- <sup>8</sup>D. L. Dheeraj, A. M. Munshi, M. Scheffler, A. T. J. van Helvoort, H. Weman, and B. O. Fimland, *Nanotechnology* **24**, 015601 (2013).
- <sup>9</sup>P. Caroff, K. A. Dick, J. Johansson, M. E. Messing, K. Deppert, and L. Samuelson, *Nat. Nanotechnol.* **4**, 50 (2009).
- <sup>10</sup>D. L. Dheeraj, G. Patriarche, H. Zhou, T. B. Hoang, A. F. Moses, S. Gronsborg, A. T. J. van Helvoort, B.-O. Fimland, and H. Weman, *Nano Lett.* **8**, 4459 (2008).
- <sup>11</sup>R. E. Algra, M. A. Verheijen, L. F. Feiner, G. G. W. Immink, W. J. P. van Enckevort, E. Vlieg, and E. P. A. M. Bakkers, *Nano Lett.* **11**, 1259 (2011).
- <sup>12</sup>R. E. Algra, M. A. Verheijen, M. T. Borgstrom, L. F. Feiner, G. Immink, W. J. P. van Enckevort, E. Vlieg, and E. P. A. M. Bakkers, *Nature* **456**, 369 (2008).
- <sup>13</sup>F. Glas, J. C. Harmand, and G. Patriarche, *Phys. Rev. Lett.* **99**, 146101 (2007).
- <sup>14</sup>S. Lehmann, J. Wallentin, D. Jacobsson, K. Deppert, and K. A. Dick, *Nano Lett.* **13**, 4099 (2013).
- <sup>15</sup>Z. Y. Lu, P. P. Chen, Z. M. Liao, S. X. Shi, Y. Sun, T. X. Li, Y. H. Zhang, J. Zou, and W. Lu, *J. Alloys Compd.* **580**, 82 (2013).
- <sup>16</sup>H. Xia, Z. Y. Lu, T. X. Li, P. Parkinson, Z. M. Liao, F. H. Liu, W. Lu, W. D. Hu, P. P. Chen, H. Y. Xu, J. Zou, and C. Jagadish, *ACS Nano* **6**, 6005 (2012).
- <sup>17</sup>X. Lu, D. A. Beaton, R. B. Lewis, T. Tiedje, and M. B. Whitwick, *Appl. Phys. Lett.* **92**, 192110 (2008).
- <sup>18</sup>A. Duzik, J. C. Thomas, A. van der Ven, and J. M. Millunchick, *Phys. Rev. B* **87**, 035313 (2013).
- <sup>19</sup>G. G. Xu, Q. Y. Wu, J. M. Zhang, Z. G. Chen, and Z. G. Huang, *Acta Phys. Sin.* **58**, 1924 (2009) (in Chinese); available at <http://wulixb.iphy.ac.cn/CN/Y2009/V58/I3/1924>.
- <sup>20</sup>P. Caroff, J. B. Wagner, K. A. Dick, H. A. Nilsson, M. Jeppsson, K. Deppert, L. Samuelson, L. R. Wallenberg, and L. E. Wernersson, *Small* **4**, 878 (2008).
- <sup>21</sup>T. C. Thomas and R. S. Williams, *J. Mater. Res.* **1**, 352 (1986).
- <sup>22</sup>J. Massies and N. Grandjean, *Phys. Rev. B* **48**, 8502 (1993).
- <sup>23</sup>G. Vardar, S. W. Paleg, M. V. Warren, M. Kang, S. Jeon, and R. S. Goldman, *Appl. Phys. Lett.* **102**, 042106 (2013).
- <sup>24</sup>J. Johansson, J. Bolinsson, M. Ek, P. Caroff, and K. A. Dick, *ACS Nano* **6**, 6142 (2012).